A New Stream Function Formulation for the Steady Euler Equations

H. L. Atkins* and H. A. Hassan†
North Carolina State University, Raleigh, North Carolina

A new stream function formulation is presented for the solution of Euler equations in the transonic flow region. In this method the stream function and the density are the dependent variables. The governing equations for adiabatic flow are then the momentum equations which are solved in the strong conservation law form. The method differs from the recent formulation of Hafez and Lovell, which is based on Crocco's equation, in that it does not require knowledge of the vorticity. To study arbitrary geometries, the algorithm is combined with the automatic grid solver (GRAPE) of Steger and Sorenson. Results are presented for an NACA 0012 airfoil at various Mach numbers, angles of attack, and cylinders. Comparisons with other solutions of the Euler equations show good agreement.

Introduction

IT has been demonstrated[1,2] that stream function formulations are capable of producing accurate and inexpensive solutions to rotational transonic flow problems. In the past, stream function methods have been based on Crocco's equation. Such an equation will model the rotational effects correctly and yield the correct shock jump condition if the correct density jump is specified. However, the method requires knowledge of the vorticity. When a shock is present, the vorticity is introduced at the shock in a discontinuous manner, resulting in numerical inaccuracies. Therefore, it is desirable to develop a stream function formulation for the Euler equations that does not require knowledge or explicit evaluation of the vorticity. Such a method has been developed herein. It is based on the strong conservation law form of Euler equations and uses the density and stream function as the dependent variables. For adiabatic flows, the governing equations reduce to the momentum equations which have no explicit dependence on the vorticity.

The resulting equations for the density and stream function can be solved in two different ways. One can add time-like terms to iterate the momentum equations. Another approach is to use an algebraic equation for the density and one or some combination of the momentum equations and solve the resulting differential equation by relaxation methods. After considerable investigation, the latter approach was selected because of its efficiency.

Solutions were obtained using various line relaxation schemes for Neumann and Dirichlet boundary conditions. It became evident during this investigation that the boundary conditions play a significant role in determining the correct lift. Thus, emphasis has been placed on investigating boundary conditions and not on developing fast solution algorithms. In spite of this, direct comparisons with an improved version[3] of FLO52, originally developed in Ref. 4, shows that the present scheme is as efficient or more efficient than FLO52.

Presented as Paper 83-1943 at the AIAA Sixth Computational Fluid Dynamics Conference, Danvers, Mass., July 13-15, 1983; received Aug. 26, 1983; revision received April 25, 1984.

*Research Assistant. Student Member AIAA.
†Professor. Associate Fellow AIAA.

Formulation of the Problem

Governing Equations and Transformations

The steady dimensionless Euler equations in general coordinates can be written as[5]

$$\frac{1}{J}\left(\frac{\partial F}{\partial \xi}+\frac{\partial G}{\partial \eta}\right)=0 \tag{1}$$

where J is the Jacobian of the coordinate transformation

$$J=x_\xi y_\eta - y_\xi x_\eta \tag{2}$$

The fluxes F and G are defined by

$$F=y_\eta \bar{F}-x_\eta \bar{G}, \qquad G=-y_\xi \bar{F}+x_\xi \bar{G} \tag{3}$$

$$\bar{F}^t=(\rho u^2+p,\rho uv,\rho u), \qquad \bar{G}^t=(\rho uv,\rho v^2+p,\rho v) \tag{4}$$

where ρ is the density, p the pressure, and u and v the velocity components in the x and y directions. The dependent variables are normalized by ρ_∞, p_∞, $(p_\infty/\rho_\infty)^{1/2}$, while the independent variables are normalized by the chord length or some other appropriate dimension. For adiabatic flows, the steady energy equation reduces to

$$T=1+[(\gamma-1)/2\gamma](\gamma M_\infty^2-u^2-v^2) \tag{5}$$

where T is the normalized temperature, γ the ratio of specific heats, and M_∞ the freestream Mach number. The equation of state

$$P=\rho T \tag{6}$$

and Eq. (5) are used to eliminate the pressure from the governing equations. In terms of the flux vectors

$$\bar{w}^t=(\rho u,\rho v,\rho) \tag{7}$$

the fluxes become

$$\bar{F}=\begin{bmatrix} \rho T_0+[(\gamma+1)(\rho u)^2-(\gamma-1)(\rho v)^2]/2\gamma\rho \\ (\rho u)(\rho v)/\rho \\ \rho u \end{bmatrix} \tag{8a}$$

$$\bar{G}=\begin{bmatrix} (\rho u)(\rho v)/\rho \\ \rho T_0+[(\gamma+1)(\rho v)^2-(\gamma-1)(\rho u)^2]/2\gamma\rho \\ \rho v \end{bmatrix} \tag{8b}$$

where T_0 is the stagnation temperature.

A stream function is introduced so that the steady continuity equation in the computational plane is satisfied exactly, i.e.,

$$\psi_\eta=\rho u y_\eta-\rho v x_\eta, \qquad \psi_\xi=\rho u y_\xi-\rho v x_\xi \tag{9}$$

This choice defines a linear transformation between the new dependent variables (ψ,ρ) and the flux vectors, and is given by

$$\begin{bmatrix} \rho u \\ \rho v \\ \rho \end{bmatrix}=\frac{1}{J}\begin{bmatrix} -x_\eta & x_\xi & 0 \\ -y_\eta & y_\xi & 0 \\ 0 & 0 & J \end{bmatrix}\begin{bmatrix} \psi_\xi \\ \psi_\eta \\ \rho \end{bmatrix}$$

or

$$\bar{W}=CW \tag{10}$$

The desired set of equations follow from Eqs. (1), (3), (8), and (10).

There are several possible approaches for solving the new system of equations. One possibility is to add time-like terms and use some explicit or implicit numerical scheme to obtain a solution. This approach proved to be a problem in that there is no obvious or natural way to put a ρ_t term back into the governing equations. Various methods have been tried but none of them proved to be successful.

Because the resulting system of equations is second order in the stream function, it is natural to investigate the use of relaxation schemes developed for the potential equation in solving this problem. This led to an investigation of equations of the type

$$\begin{bmatrix} -\alpha_1 & \alpha_2 \\ \alpha_2 & \alpha_1 \end{bmatrix}\begin{bmatrix} x\text{ momentum} \\ y\text{ momentum} \end{bmatrix}=0 \tag{11}$$

For the case where

$$\alpha_1=\sin\theta, \quad \alpha_2=\cos\theta, \quad \tan\theta=v/u \tag{12}$$

the first equation

$$H(\psi,\rho)=\cos\theta\,(y\text{ momentum})-\sin\theta\,(x\text{ momentum}) \tag{13}$$

reduces to Crocco's equation

$$q(v_x-u_y)=(T/q)(uS_y-vS_x), \qquad q=(u^2+v^2)^{1/2} \tag{14}$$

S is the entropy (dimensional entropy divided by the gas constant) defined by

$$T\mathrm{d}S=\frac{\gamma\mathrm{d}T}{\gamma-1}-\frac{\mathrm{d}P}{\rho} \tag{15}$$

The second equation reduces to the statement that S is constant along a streamline, i.e.,

$$u\frac{\partial S}{\partial x}+v\frac{\partial S}{\partial y}=0 \tag{16}$$

Integrating Eq. (15), one finds

$$\rho=T^{1/\gamma-1}\exp(S_\infty-S) \tag{17}$$

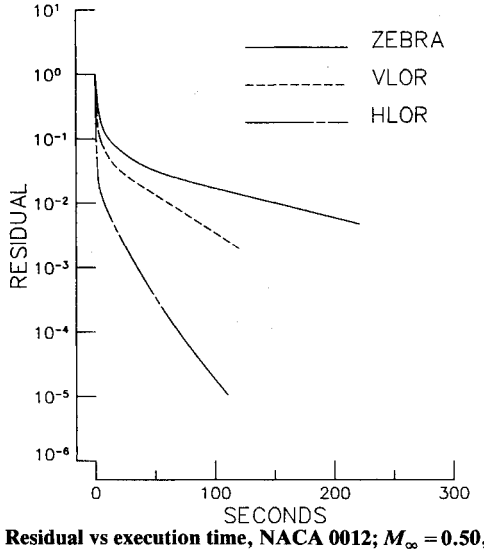

Fig. 2 Residual vs execution time, NACA 0012; $M_\infty=0.50$, $\alpha=2.0$.

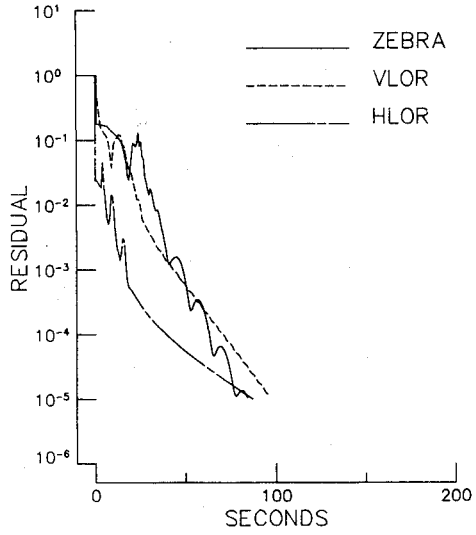

Fig. 1 Residual vs execution time, NACA 0012; $M_\infty=0.84$, $\alpha=0.0$.

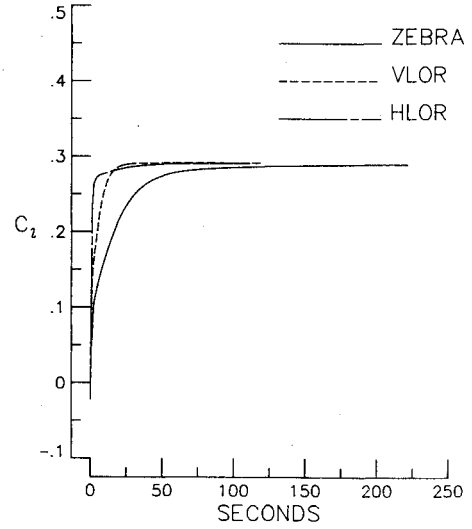

Fig. 3 C_l vs execution time, NACA 0012; $M_\infty=0.50$, $\alpha=2.0$.

The entropy jump at the shock is obtained from the Rankine-Hugoniot jump condition

$$\exp(S-S_\infty)=\left[\frac{2}{(\gamma-1)M_n^2}+\frac{\gamma-1}{\gamma+1}\right]^{\frac{\gamma}{\gamma-1}} \times\left[\frac{2\gamma}{\gamma+1}M_n^2-\frac{\gamma-1}{\gamma+1}\right]^{\frac{1}{\gamma-1}} \tag{18}$$

where M_n is the normal Mach number before the shock. Thus, the equations governing the (ψ,ρ) formulation of the Euler equations reduce to Eqs. (13) and (17). Note that Eq. (13) does not have any source terms.

Although this approach reduces the Euler equations to one differential equation for the stream function and one algebraic equation for the density, the latter introduces an old difficulty.[1,2] Equation (17) gives two values of ρ for a given mass flux. Special treatment is necessary to prevent the formation of expansion shocks at the sonic point. This has been achieved by employing artificial density methods.

Method of Solution

Starting with an initial estimate of ψ, ρ, and $\bar{\rho}$ an algorithm was developed to calculate ψ and ρ. The iterative scheme for ψ has the form

$$L\Delta\psi=-wH(\psi^n,\rho^n) \tag{19}$$

where w is a relaxation factor. Updates of the various properties are given as

$$\psi^{n+1}=\psi^n+\Delta\psi \tag{20a}$$

$$\bar{\rho}^{n+1}=\bar{\rho}^n(1-w_1)+w_1(\rho-\mu\Delta\xi\rho_\xi)^n \tag{20b}$$

$$u^{n+1}=(-x_\eta\psi_\xi^{n+1}+x_\xi\psi_\eta^{n+1})/J\bar{\rho}^{n+1} \tag{20c}$$

$$v^{n+1}=(y_\xi\psi_\eta^{n+1}-y_\eta\psi_\xi^{n+1})/J\bar{\rho}^{n+1} \tag{20d}$$

$$T^{n+1}=T(u^{n+1},v^{n+1}) \tag{20e}$$

$$\rho^{n+1}=w_2(T^{n+1})^{1/\gamma-1}\exp(S-S_\infty)+(1-w_2)\rho^n \tag{20f}$$

The entropy is updated with each iteration by locating the shock, if one exists, and calculating the shock strength. A table of shock strength vs stream function is generated and is used to calculate the entropy downstream of the shock. Upstream of the shock the entropy is equal to the freestream value, and w_1 and w_2 are relaxation factors.

Because Eq. (13) reduces to a Poisson-type equation, its solution can be obtained using relaxation schemes. Three methods—HLOR, VLOR, and Vertical Zebra—were employed and compared. The form of the left-hand side of Eq. (19) depends on the particular scheme being used. The Newton coefficients are easily determined from the Jacobians of F and G and the linear transformation given in Eq. (10). A detailed description of the implementation of the various schemes can be found in Ref. 6.

Each of the preceding schemes involves solving tridiagonals in one direction. For HLOR, the tridiagonal is along an $\eta=$ const line; it starts one line off the body and proceeds outward. For both VLOR and Zebra, the tridiagonal is along a $\xi=$ const line. In VLOR the sweep begins upstream and proceeds downstream. The Zebra scheme is performed in two sweeps; the first sweep solves even lines and the second sweep solves odd lines. In this method, the direction of the sweep is not critical. All airfoil calculations were performed on C-grids which have a cut in the wake region. In all of these schemes the tridiagonals were structured so that the wake could be solved implicitly.

Difference Operators

The right-hand side of Eq. (19) is evaluated in terms of the primitive variables as

$$H(\psi^n,\rho^n)\equiv E(\rho^n,u^n,v^n) \equiv\cos\theta\,(y\text{ momentum})-\sin\theta\,(x\text{ momentum}) \tag{21}$$

The momentum equations were differenced using the three-point type-dependent operator developed in Ref. 5. Thus,

$$\frac{\partial}{\partial\xi}Q_{ij}=\frac{1}{\Delta\xi}\,\frac{\mu\delta-(\beta/2)\nabla(\epsilon_{ij}\Delta)+[(1-\beta)/2]\Delta(\epsilon_{ij}\nabla)}{1-(\beta/2)\nabla\epsilon_{ij}+[(1-\beta)/2]\Delta\epsilon_{ij}}\,Q_{ij} \tag{22}$$

where

$$\mu\delta Q_{ij}=\tfrac{1}{2}(Q_{i+1,j}-Q_{i-1,j})$$

$$\nabla Q_{ij}=Q_{i,j}-Q_{i-1,j},\quad \Delta Q_{ij}=Q_{i+1,j}-Q_{i,j}$$

$$\epsilon_{i,j}=1, M_{i,j}>1,\qquad \beta=1,\text{ upper surface}$$

$$=0, M_{i,j}\le 1,\qquad =0,\text{ lower surface} \tag{23}$$

A central difference operator is used in the η direction.

In the present work the artificial density shifts only in the ξ direction. The $\Delta\xi\rho_\xi$ term in Eq. (20b) is evaluated using a first-order upwind difference scheme

$$\Delta\xi\rho_\xi=\rho_i-\rho_{i-1},\qquad u>0$$

$$=\rho_i-\rho_{i+1},\qquad u<0 \tag{24}$$

The coefficient μ is of the form

$$\mu=\mu_0\max\{1-(M_s/M)^2,\ 0\}$$

where μ_0 and M_s are constants.

Central difference operators are used to evaluate the derivatives indicated in Eqs. (20c) and (20d)

$$\psi_\xi=(1/2\Delta\xi)(\psi_{i+1,j}-\psi_{i-1,j})$$

$$\psi_\eta=(1/2\Delta\eta)(\psi_{i,j+1}-\psi_{i,j-1}) \tag{25}$$

It should be noted that the choice of operators used in the update relations determines the form of the continuity equation being satisfied. In view of Eq. (25), the continuity equation is satisfied by the use of three-point central difference operators, not by the type-dependent operator used for the momentum equations.

A different set of operators is required for the left-hand side of Eq. (19) to maintain the tridiagonal structure. Terms of the form

$$\frac{\partial}{\partial\xi}\left(a\,\frac{\partial\Delta\psi}{\partial\xi}\right)$$

are evaluated as

$$\left(\frac{a_{i-1}+a_i}{2}\right)\Delta\psi_{i-1,j}-\left(\frac{a_{i-1}+2a_i+a_{i+1}}{2}\right)\Delta\psi_{i,j} +\left(\frac{a_i+a_{i+1}}{2}\right)\Delta\psi_{i+1,j}$$

As an example, applying the above difference operators to the case of HLOR for $\beta=1$ gives the difference equation shown in the Appendix.

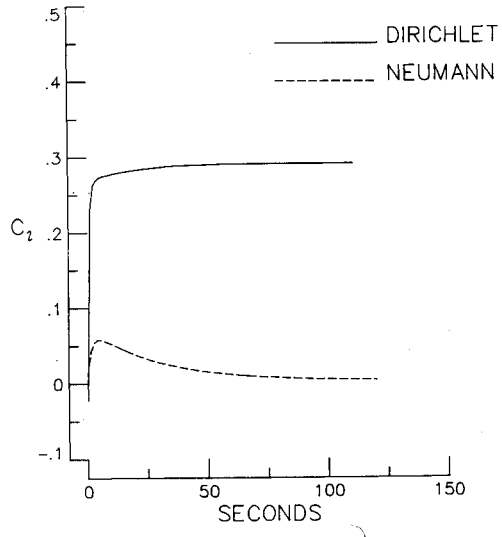

Fig. 4 C_l vs execution time, NACA 0012; $M_\infty = 0.50$, $\alpha = 2.0$.

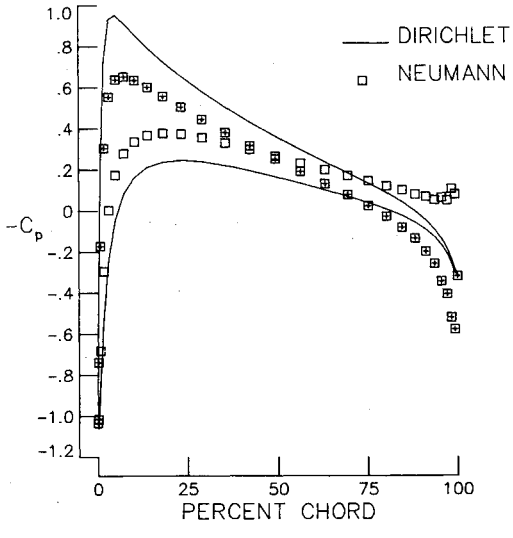

Fig. 5 C_p vs percent chord. Effect of far-field boundary condition, NACA 0012; $M_\infty = 0.50$, $\alpha = 2.0$.

Boundary Conditions

One of the advantages of the stream function formulation is that some boundary conditions become simple to implement. The tangency condition, for instance, is expressed by specifying $\psi = \text{const}$ on the body. For C-grids, the Kutta condition is easily implemented by setting ψ on the body equal to ψ at the first point off the trailing edge. When the entropy at the trailing edge is treated properly this is equivalent to requiring continuity of pressure.

Some care must be taken to insure that the far-field boundary condition does not conflict with the body boundary condition. Far from the body, the stream function approximates that of a vortex and doublet in uniform flow. Thus, for low speeds one can write

$$\psi = u_\infty (y\cos\alpha - x\cos\alpha) + m/R + \Gamma \ell nR + c$$

$$\psi_\eta = u_\infty (y_\eta \cos\alpha - x_\eta \sin\alpha) + \frac{1}{R^2}\left(\Gamma - \frac{m}{R}\right)(xx_\eta + yy_\eta)$$

$$R^2 = x^2 + y^2 \qquad (26)$$

where α is the angle of attack and m, Γ, and c are constants. In most cases the doublet term is sufficiently small and can be ignored. For O-grids and certain C-grids, the ℓnR term is constant or nearly constant. Because Γ is constant for a particular flow, it is always possible to choose a "c" that will cancel the vortex term. Hence, a valid Dirichlet boundary condition for both lifting and nonlifting cases is simply

$$\psi = u_\infty (y\cos\alpha - x\sin\alpha) \qquad (27)$$

Thus, a Dirichlet boundary condition places a constraint on the influx and outflux of the mass but not on the lift.

The Neumann boundary condition, on the other hand, has a strong influence on the lift. The vortex term is of the order $1/R$. However, it can never be neglected in lifting cases because the circulation depends on the integral of ψ_η around the outer boundary, which is of the order R. Neglecting the vortex term has the effect of specifying the circulation, and, consequently, the lift, to be zero. Thus, when a Neumann boundary condition is used for lifting bodies, the circulation must be calculated by some means and specified at the outer boundary.

Results and Discussion

The method developed is used to study the flow past airfoils at various angles of attack, Mach numbers, and cylinders. To facilitate comparisons with other airfoil calculations, results are given for NACA 0012 only. Unless indicated otherwise, the airfoils are mapped by a C-grid with 79×25 points and the cylinder is mapped by an O-grid with 79×23 points. The C-grids were generated by the GRAPE program.

Figures 1-3 indicate the effect of the method of solution on convergence. The execution time is the CPU time on the CYBER 203, however, none of the algorithms have been vectorized. It is seen from Fig. 1 that if the convergence criterion is based on a value for the residual of 10^{-3} or higher, then HLOR is superior. On the other hand, if the convergence criterion is based on a residual of 10^{-5} or lower, then Zebra is superior. Although Fig. 1 shows that all three schemes have similar convergence histories at zero angle of attack, Fig. 2 shows that the convergence history of the three methods depends, to a large extent, on the angle of attack. Figure 3 shows that the scheme which reduces the residual the quickest also converges to the steady lift coefficient the fastest. However, when considering Figs. 2 and 3, it becomes clear that reduction of the residual by a specified order of magnitude is not necessarily the best convergence criterion. It should be noted that, when lifting bodies are considered, the schemes that employ vertical line over-relaxation are the slowest to converge.

Figures 4 and 5 indicate the importance of specifying the correct far-field boundary conditions. It is clear from Fig. 4 that a Neumann boundary condition that does not take into consideration the asymptotic behavior of the solution at the large distance from the body yields the wrong lift. This is in spite of the fact that it meets a convergence criterion based on the residual. The strange behavior of C_p indicated in Fig. 5 for the case of Neumann boundary conditions is a consequence of specifying the far-field circulation to be zero.

Figure 6 shows the effect of the mesh size on pressure distribution for a cylinder at $M = 0.45$. It is seen that 39 cells around the cylinder give satisfactory results.

Figure 7 shows the effect of artificial density on the pressure distribution. Although the magnitude of μ_0 does not affect the position of the shock, it does affect the Mach number ahead of the shock. Moreover, higher values of μ_0 are needed to achieve convergence for finer grids. This appears to be the only drawback of the method.

Figures 8-10 compare the predictions of this theory for NACA 0012 with FLO52-S, the newest version of FLO52 described in Ref. 3, while Fig. 11 compares the present method with FLO52-S and Steger's method[8] for a cylinder at $M_\infty = 0.45$. It should be noted that Fig. 10 employs a 158×25

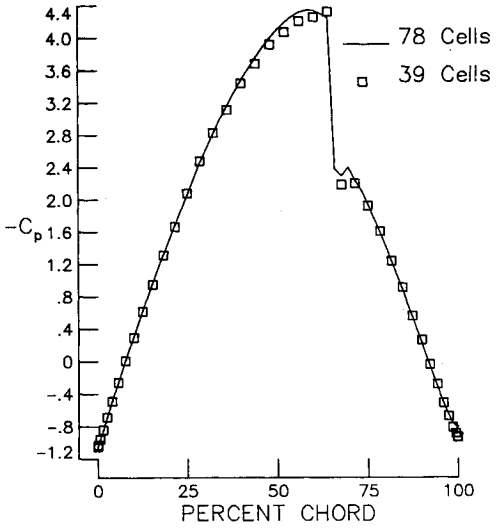

Fig. 6 C_p vs percent chord. Effect of mesh size, cylinder, $M_\infty = 0.45$.

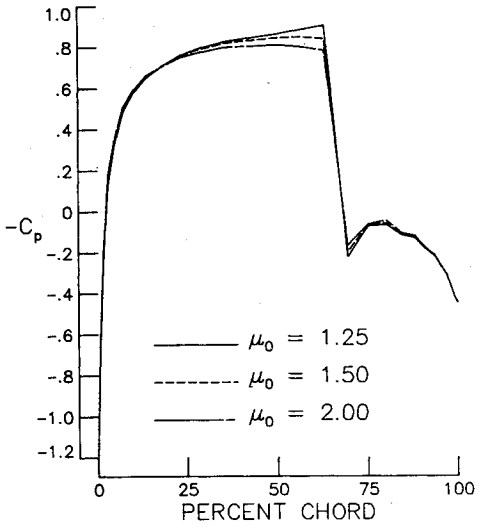

Fig. 7 C_p vs percent chord. Effect of artificial density, NACA 0012; $M_\infty = 0.84$.

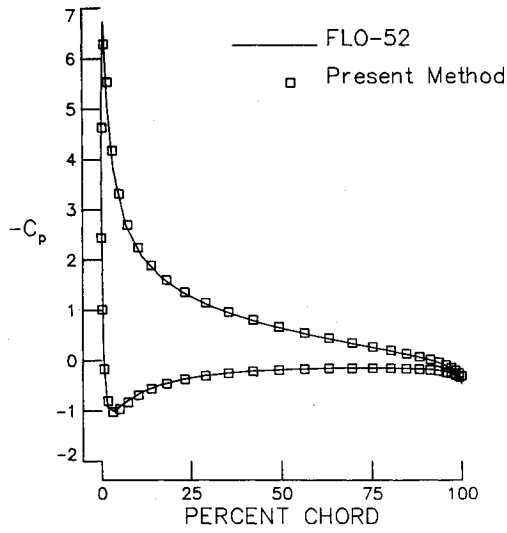

Fig. 8 C_p vs percent chord, NACA 0012; $M_\infty = 0.30$, $\alpha = 10.0$.

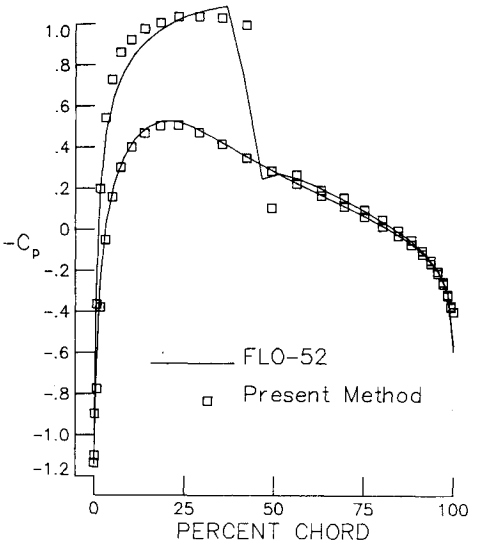

Fig. 9 C_p vs percent chord, NACA 0012; $M_\infty = 0.76$, $\alpha = 1.0$.

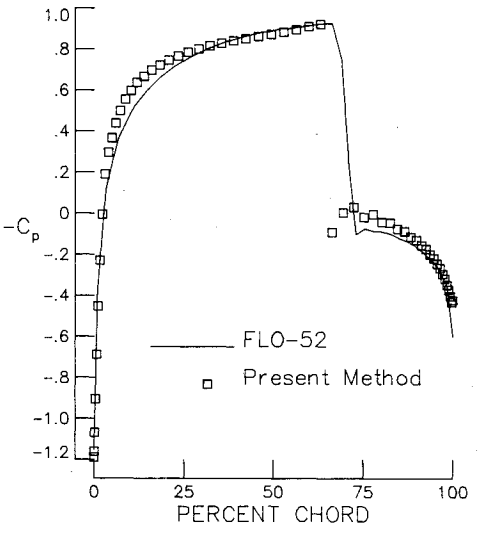

Fig. 10 C_p vs percent chord, NACA 0012; $M_\infty = 0.84$.

C-grid. All airfoil comparisons with FLO52-S, which employ 120×33 O-grids, were provided by Salas,[9] while the cylinder comparisons were provided by Wornom,[10] both from the NASA Langley Research Center. Figure 8 shows that the present method, which for $M_\infty = 0.3$ does not have any smoothing, is in excellent agreement with FLO52-S. Figures 9 and 10 show that the present method has an overexpansion in the neighborhood of the sonic line. This results from the use of artificial density to prevent the expansion shock and can be improved by calculating density as suggested in Ref. 2. Otherwise, the solutions are in good agreement for both airfoils and cylinders. However, as seen from Fig. 11, this method is not in good agreement with Steger's method in the supersonic region. The spike preceding the shock in Steger's method may be traced to the use of central difference operators and an explicit smoothing term with a constant coefficient.

Finally, Fig. 12 compares the speed of computation of this method with that of FLO52-S. It is seen from Fig. 12 that if the convergence criterion is based on a reduction of the residual by three orders of magnitude, then the two methods are competitive. On the other hand, if the convergence criterion is based on a reduction of the residual by five orders of magnitude or more, then the present method is superior.

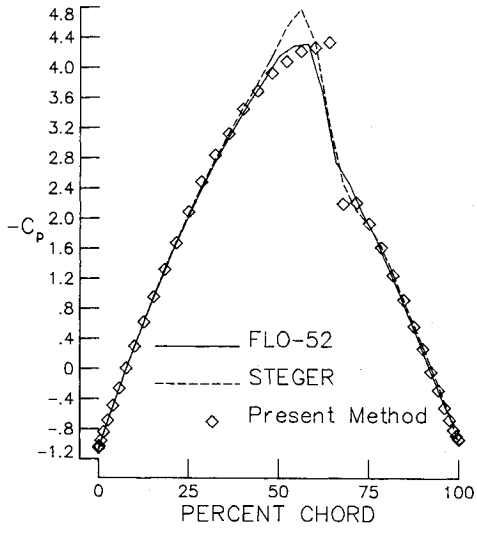

Fig. 11 C_p **vs percent chord cylinder;** $M_\infty = 0.45$.

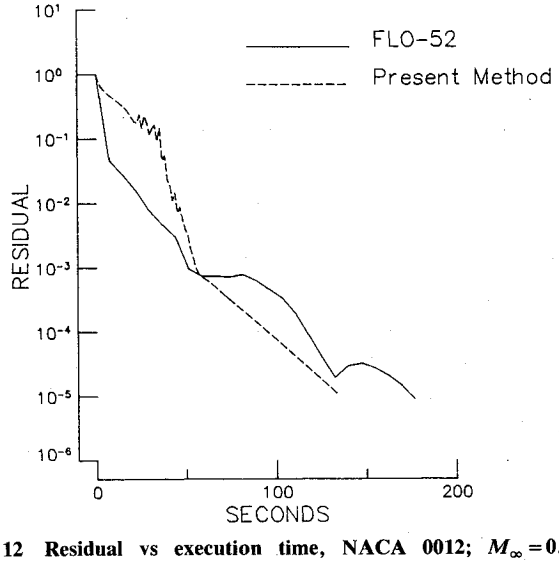

Fig. 12 Residual vs execution time, NACA 0012; $M_\infty = 0.84$, $\alpha = 0.0$.

Concluding Remarks

The predictions of the stream function approach developed here are in good agreement with FLO52-S. In spite of the fact that no attempt has been made to accelerate the computation, comparison of the CPU time for both schemes shows that, in general, the present method is more efficient. It has been demonstrated that stream function calculations in three dimensions are practical for isentropic flow. The extension of the present algorithm is straightforward; however, the method of determining entropy as a function of two stream surfaces may become cumbersome. Therefore, it is felt that solutions of the Euler equations based on stream function formulations are both accurate and inexpensive and, thus, deserve further attention.

Appendix: Application of Finite Difference Operator for the Case of HLOR and $\beta = 1$

The linearized equation has the form

$$[-\sin\theta_{ij}, \cos\theta_{ij}]\,[(V^1_{ij}\Delta\psi_\xi)_\xi + (V^2_{ij}\Delta\psi_\xi)_\xi]$$

$$= [\sin\theta_{ij}, -\cos\theta_{ij}]\,[F_\xi + G_\eta]$$

where

$$V^1 = \frac{\partial F}{\partial \psi_\xi} \quad \text{and} \quad V^2 \equiv \frac{\partial G}{\partial \psi_\xi}$$

Replacing derivatives with the difference operator previously described gives

$$[-\sin\theta_{ij}, \cos\theta_{ij}]\left[\frac{V^1_{i+1,j}+V^1_{i,j}}{2}\Delta\psi_{i+1,j} - \left(\frac{V^1_{i+1,j}+2V^1_{i,j}+V^1_{i-1,j}}{2}\right.\right.$$

$$\left.\left. + \frac{V^2_{i,j+1}+2V^2_{i,j}+V^2_{i,j-1}}{2}\right)\Delta\psi_{ij} + \frac{V^1_{i-1,j}+V^1_{i,j}}{2}\Delta\psi_{i-1,j}\right]$$

$$= \omega[\sin\theta_{ij}, -\cos\theta_{ij}]\left[\frac{V^2_{i,j}+V^2_{i,j-1}}{2}\Delta\psi_{i,j-1} + \frac{(1-\epsilon_{i,j})}{2}F_{i+1,j}\right.$$

$$+ \frac{(\epsilon_{i,j}+\epsilon_{i+1,j})}{2}F_{i,j} - \frac{(1+\epsilon_{i-1,j})}{2}(G_{i,j+1}-G_{i,j-1})$$

$$\left. + \frac{\epsilon_{i-1,j}}{4}(G_{i-1,j+1}-G_{i-1,j-1})\right]$$

where

$$\epsilon_{i,j} = 1, \quad M_{i,j} > 1$$

$$= 0, \quad M_{i,j} \le 1$$

and ω is the relaxation factor.

Acknowledgments

Part of this work was carried out while the authors were at the Theoretical Aerodynamics Branch of the NASA Langley Research Center. The authors would also like to acknowledge many helpful discussions with members of the branch and especially with Jerry South, Mohamed Hafez, and Manny Salas. This work was supported in part by NASA Cooperative Agreement NCCI-22.

References

[1]Emmons, H., "Flow of a Compressible Fluid Past a Symmetric Airfoil in a Wind Tunnel and in Free Air," NASA TN 1746, 1984.

[2]Hafez, M. and Lovell, D., "Numerical Solution of Transonic Stream Function Equation," *AIAA Journal*, Vol. 21, March 1983, pp. 327-335.

[3]Salas, M. D., Jameson, A., and Melnik, R. E., "A Comparative Study of the Nonuniqueness Problem of the Potential Equation," AIAA Paper 83-1888, July 1983.

[4]Jameson, A., Schmidt, W., and Turkel, E., "Numerical Solutions of the Euler Equations by Finite Volume Methods Using Runge-Kutta Time-Stepping Schemes," AIAA Papr 81-1259, June 1981.

[5]Atkins, H. L. and Hassan, H. A., "Transonic Flow Calculations Using Euler's Equations," *AIAA Journal*, Vol. 21, June 1983, pp. 842-847.

[6]Hafez, M. M. and Lovell, D. R., "Improved Relaxation Schemes for Transonic Potential Calculations," AIAA Paper 83-0372, Jan. 1983.

[7]Steger, J. L. and Sorenson, R. L., "Automatic Mesh Point Clustering Near a Boundary in Grid Generation with Elliptic Partial Differential Equations," *Journal of Computational Physics*, Vol. 33, Dec. 1979, pp. 405-410; also, NASA TM 81198, May 1980.

[8]Steger, J. L., "Implicit Finite-Difference Simulation of Flow About Arbitrary Two-Dimensional Geometries," *AIAA Journal*, Vol. 16, July 1978, pp. 679-686.

[9]Salas, M. D., Personal communication, NASA Langley Research Center, Hampton, Va., April 1983.

[10]Wornom, S., Personal communication, NASA Langley Research Center, Hampton, Va., April 1983.

[11]Sherif, A. and Hafez, M., "Computation of Three Dimensional Transonic Flows Using Two Stream Functions," AIAA Paper 83-1948, July 1983.